

# Wavelet-based Neuroelectromagnetic Source Estimation

Richard E. Greenblatt\* and Allen Osman<sup>§</sup>

\*Source Signal Imaging, San Diego CA 92012 USA

<sup>§</sup>Department of Psychology, University of Pennsylvania,  
Philadelphia PA 10104

[www.sourcesignal.com](http://www.sourcesignal.com)

## 1 Summary

A method is described for estimating electrical source currents from wavelet-transformed multichannel electromagnetic encephalographic (EMEG) scalp data. The methods have been validated using simulations and evaluated with experimental evoked response data.

## 2 Introduction

The longstanding interest in EEG-recorded oscillatory events begins with the pioneering work of Berger (1929). It has seen recent renewed attention with experimental and theoretical studies linking coherent multicellular rhythms with cognitive events (e.g. Gray *et al.*, 1989; Ribary *et al.*, 1991), and through the investigation of event related desynchronization (recently reviewed in Pfurtscheller and Lopes da Silva 1999). Conventional Fourier transform methods (e.g FFT) are not well suited for the analysis of transient oscillations, since FFT's assume statistical stationarity, and, in addition have no time resolution. Time-frequency analysis using the Wigner transform (Morgan and Gevins, 1986) or wavelets (Bertrand *et al.*, 1996) overcomes some of the limitations of conventional FFT's, permitting simultaneous time-based and frequency-based analysis of the EEG signal. Wavelets have well developed mathematical foundations (e.g. Meyer, 1993), and have become the method of choice for EMEG time/frequency analysis. Several groups have applied time frequency analysis to the study of evoked potential (Tallon-Baudry *et al.*, 1996) and evoked magnetic field data (Bertrand *et al.*, 1996), but to the best of my knowledge,

no methods have been published for obtained electromagnetic source estimates from wavelet transformed MEG data.

## 2.1 Time-frequency analysis

Complex Grossmann-Morlet wavelets,  $w(t, f_c) = A e^{-\frac{t^2}{2\sigma_t^2}} e^{2i\pi f_c t}$ , are Gaussian in both time and frequency, where  $t$ =time,  $f_c$ =center frequency,  $\sigma_t$  is the temporal dispersion, and  $A = \left(\sigma_t \sqrt{\pi}\right)^{-\frac{1}{2}}$  is a normalization factor such that the total energy is 1 (Kronland-Martinet *et al.*, 1987). Then for a single channel time series  $s(t)$ , we can obtain an estimate of the time-varying frequency component at  $f_c$  as  $y(t, f_c) = \{s(t) \cdot w(t, f_c)\}$ , where  $\{\cdot\}$  represents the convolution operator. By successive applications at differing center frequencies, a time/frequency map may be constructed for one or several channels. This is displayed diagrammatically in Figure 1A. For evoked response data, convolution may be applied to the averaged time series, or to the individual epochs, averaging after convolution (Tallon-Baudry *et al.*, 1996). The former extracts phase-locked components, while the later is insensitive to phase locking. This is displayed diagrammatically in Figure 1B. Lastly, we note that since phase information is preserved in the convolution, the resultant complex-valued map may be used for source estimation.

## 2.2 Source estimation

Because the total and non-phase-locked components may only be computed by introducing a nonlinear step, the phase information required for source estimation (Lütkenhöner, 1992) is lost. We address this by mapping the complex-valued wavelet coefficients for each trial from signal to source space using an inverse operator. Then we can compute the total, phase-locked, and non-phase locked components by summing over trials in source space, obtaining the desired inverse estimate.

Given  $M \in \mathbb{N}$  channels and  $T \in \mathbb{N}$  sampled time points, we define a measurement matrix  $\mathbf{M} \in \mathbb{C}^{M \times T}$ . With each channel we associate a sensor (electric or magnetic), with known location and sensitivity on or outside the head. Assume a source space  $\mathbf{Q} = \mathbb{C}^N$ , consisting

of  $N \in \mathbb{N}$  complex-valued dipoles, each fixed in location (e.g. on the sampled cortical surface). Let  $\mathbf{G} : \mathbf{Q} \rightarrow \mathbf{M}$  be the matrix representation of the forward operator, with generalized inverse  $\mathbf{G}^\oplus$ . Note that  $\mathbf{G}$  (and  $\mathbf{G}^\oplus$ ) are real, due to the quasi-static approximation.

### 3 Analytical methods

Define the power for a single wavelet coefficient as  $S^2(y) = yy^*$ , where  $y^*$  is the complex conjugate of  $y$ . The power vector  $\mathbf{S}^2(\mathbf{y})$  is defined in the obvious way, on an element-by-element basis. For  $I$  trials, the mean total power is

$$\bar{\mathbf{S}}_{\text{total}}^2(\mathbf{y}_0, \dots, \mathbf{y}_{I-1}) = \frac{1}{I} \sum_I \mathbf{S}^2(\mathbf{y}_i) \quad (1)$$

The mean *phase-locked* power is

$$\bar{\mathbf{S}}_{\text{locked}}^2(\mathbf{y}_0, \dots, \mathbf{y}_{I-1}) = \mathbf{S}^2\left(\frac{1}{I} \sum_I \mathbf{y}_i\right) \quad (2)$$

Note that since  $\mathbf{S}^2$  is nonlinear in  $\mathbf{y}$ , in general,  $\bar{\mathbf{S}}^2(\mathbf{y}_0, \dots, \mathbf{y}_{I-1}) \neq \bar{\mathbf{S}}_{\text{locked}}^2(\mathbf{y}_0, \dots, \mathbf{y}_{I-1})$ . In fact, their difference defines the mean *induced* power as

$$\bar{\mathbf{S}}_{\text{induced}}^2 = \bar{\mathbf{S}}_{\text{total}}^2 - \bar{\mathbf{S}}_{\text{locked}}^2 \quad (3)$$

Equations (1)-(3) define wavelet power in measurement space. Using the generalized inverse,  $\mathbf{G}^\oplus$ , we can estimate the source space wavelet power as

$$\hat{\mathbf{S}}_{\text{Q,total}}^2 = \frac{1}{I} \sum_I \mathbf{S}^2(\mathbf{G}^\oplus \mathbf{y}_i) \quad (4)$$

$$\hat{\mathbf{S}}_{\text{Q,locked}}^2 = \mathbf{S}^2\left(\frac{1}{I} \sum_I \mathbf{G}^\oplus \mathbf{y}_i\right) = \mathbf{S}^2\left(\mathbf{G}^\oplus \left(\frac{1}{I} \sum_I \mathbf{y}_i\right)\right) \quad (5)$$

$$\hat{\mathbf{S}}_{\text{Q,induced}}^2 = \hat{\mathbf{S}}_{\text{Q,total}}^2 - \hat{\mathbf{S}}_{\text{Q,locked}}^2 \quad (6)$$

## 4 Validation

### 4.1 Methods

The analytic methods were coded in C++ and incorporated into EMSE Suite software (Source Signal Imaging, San Diego CA) for verification and evaluation. The methods and implementation were verified with simulations, and evaluated with experimental data.

## 4.2 Simulations

Simulations may be used to validate the algorithm implementation under controlled conditions, where the correct answer is known. This permits us to verify that inverting the wavelet coefficient topographic map will find true location in a simple (noise free, no modeling error) case.

A multichannel time series was created by summing the signals obtained from 2 simulated dipolar sources, one phase-locked and one non-phase-locked. These simulated source time series, at specified location on spherical surface interior to 3-shell sphere, were projected analytically to the surface of the 3-shell sphere. The resulting time series were analyzed into their wavelet components, and the source estimates for these components compared to the known dipole locations, as shown in Figure 2.

## 4.3 Experimental Data

### 4.3.1 Purpose

Experimental data may be used to evaluate the code implementation under realistic conditions where the true answer is not known, but where plausible locations may be determined *a priori*.

### 4.3.2 Methods

As part of another study, 59 channel electrical recordings were obtained from 16 subjects during rhythmic finger tapping. Individual trials were averaged within subjects, and grand averages were obtained. The grand averages were wavelet transformed, computing cortical current source density estimates on the outer surface of an average brain, as shown in Figure 3. The wavelet-based source estimates were obtained and compared to the source estimates derived from the FT data (not shown).

## 5 Conclusions

- We have developed analytic methods to obtain source estimates for phase-locked and non-phase locked wavelet-transformed EMEG data.
- In simulations, phase-locked and non-phase-locked components could be separately identified from the time series mixture, and their individual sources correctly localized.

- Using experimental data, both phase-locked and non-phase-locked components could be identified in the grand average data. The sources localized to physiologically plausible locations, and these wavelet-derived source locations corresponded to locations obtained from grand average data using non-wavelet-based methods.

## 6 Literature cited

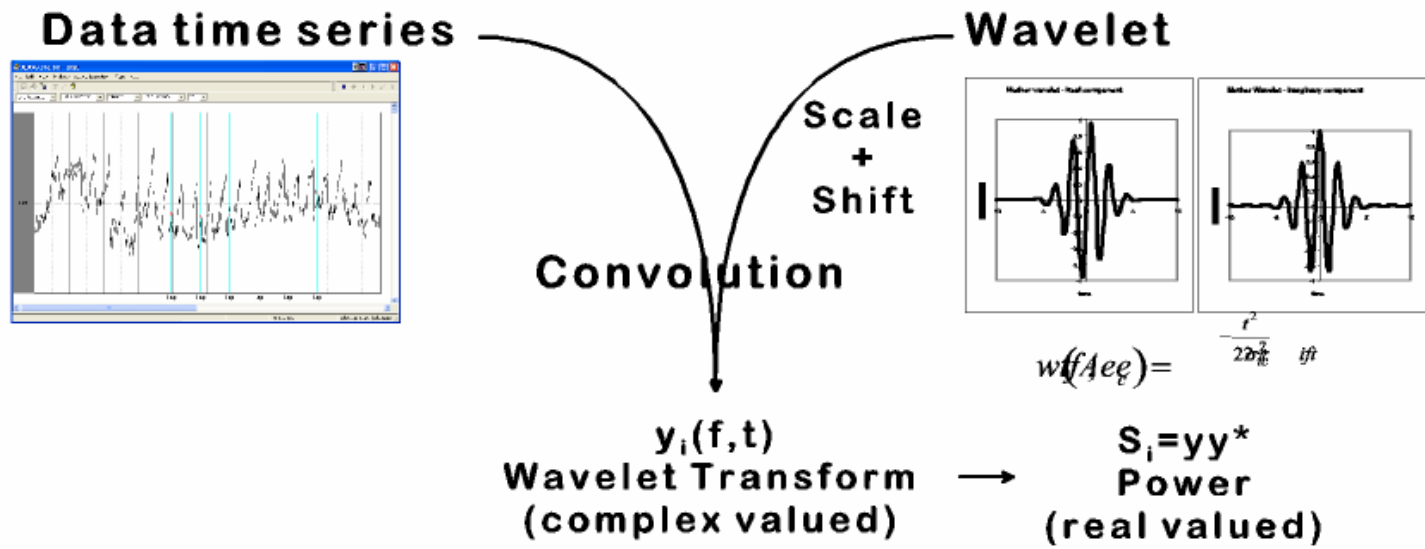
- Berger, H. Über das Elektrokephalogramm des Menschen. II. *Archiv für Psychiatrie und Nervenkrankheiten*, **87**:525-570 (1929).
- Bertrand O, Tallon-Baudry C, and Pernier J. Time-frequency analysis of oscillatory gamma-band activity: wavelet approach and phase-locking estimation. in Aine, C., Okada, Y., Stroink, G., Swithenby, S., and Wood, C. (Eds.), *Advances in Biomagnetism Research: Biomag96*, Springer-Verlag, New York, (2000).
- Gray CM, Engel AK, König P, and Singer, W. Oscillatory responses in cat visual cortex exhibit inter-columnar synchronization which reflects global stimulus properties. *Nature* **338**:334-337. 1989.
- Kronland-Martinet R, Morlet J, and Grossmann, A. Analysis of sound patterns through wavelet transforms. *Intl. J. Pattern Recog. Artificial Intelligence* **1**:273-302. 1987.
- Lütkenhöner, B. Frequency-domain localization of intracerebral dipolar sources. *EEG. Clin. Neurophysiol.* **82**(1992) 112-118.
- Meyer Y. *Wavelets: algorithms and applications*. SIAM (Philadelphia) 1993.
- Morgan NH and Gevins AS. Wigner Distributions of Human Event-related brain potentials. *IEEE Trans. BME* **33**:63-70. 1986.
- Pfurtscheller G and Lopes da Silva FH. *Event-Related Desynchronization, Handbook of Electroencephalography and Clinical Neurophysiology* **6**, Elsevier, Amsterdam (1999).
- Ribary U, Ioannides AA, Singh KD, Hasson R, Bolton JPR, Lado F, Molginer A, and Llinas R. Magnetic tomography of coherent thalamocortical 40-Hz oscillations in humans. *Proc. Natl. Acad. Sci. USA* **88**:11037-11041. 1991.
- Tallon-Beaudry, C, Bertrand, O, Delpuech, C, and Pernier, J. Stimulus Specificity of Phase-Locked and Non-Phase-Locked 40 Hz Visual Responses in Human. *J. Neurosci.* **16**(1996):4240-4249.
- Torrance C and Compo GP. A Practical Guide to Wavelet Analysis. *BAMS* **79**(1998):61-78.

## 7 Acknowledgements

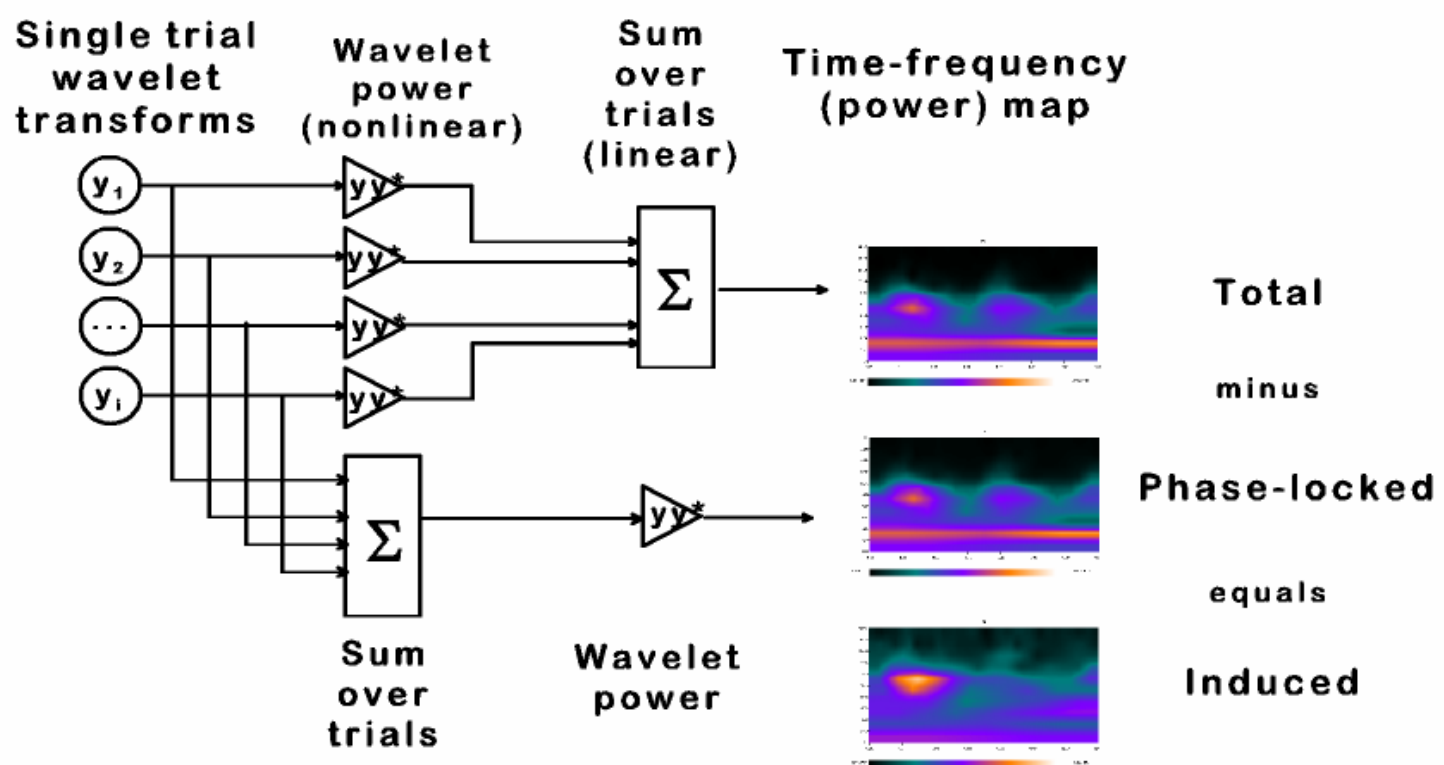
This work was supported in part by US NIH grant NS36133 to REG and NS37528 to AO, whose support is gratefully acknowledged.

## Analysis method - wavelet transform

### A. Single trial - signal space



### B. Multiple trials - signal space



### C. Multiple trials - source space

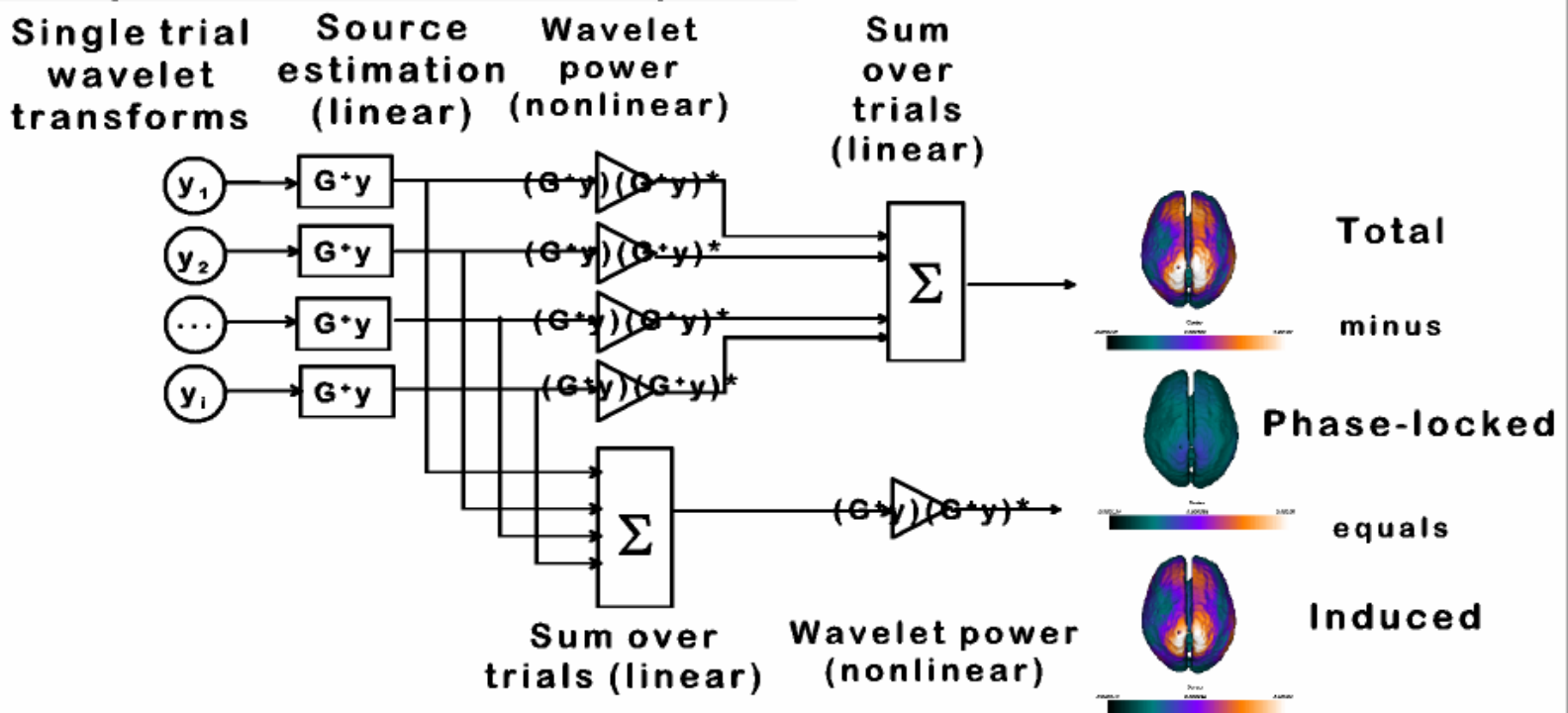


**Figure 1.** (A) Convolution of scaled and shifted mother wavelet with data time series yields the signal space wavelet transform. (B) Single trial wavelet transforms may be summed before or after converting to power to yield the total, phase locked, and induced components ( equations 1-3). (C) Transforming wavelet coefficients to source space before squaring yields phase-locked and induced current density estimates.(equations 4-6).

## Wavelet-based source estimation - simulation

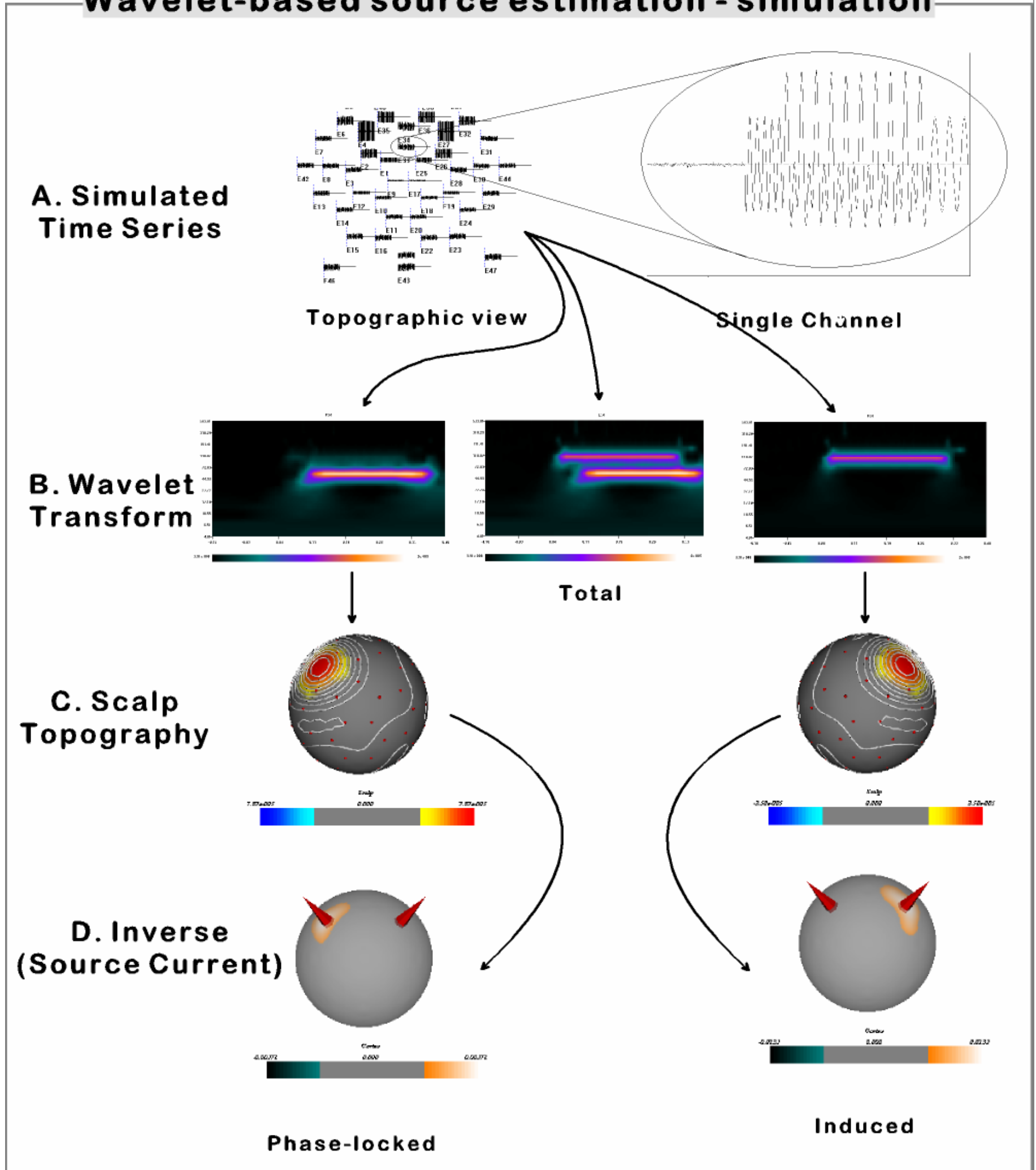


**Figure 2.** (A) A multichannel time series was created by summing the signals obtained from 2 simulated dipolar sources, one phase-locked and one non-phase-locked, over 8 trials. These simulated source time series, at specified location on spherical surface interior to 3-shell sphere, were projected analytically to the surface of the 3 shell sphere. (B) The resulting source time series were analyzed into their wavelet components. A time-frequency window was selected and the resulting scalp topography (C) was used for source estimation. (D) The source estimates for these components may be compared to the known dipole locations (location represented by the cone base and orientation by the cone apex).

## Wavelet-based source estimation - experimental data

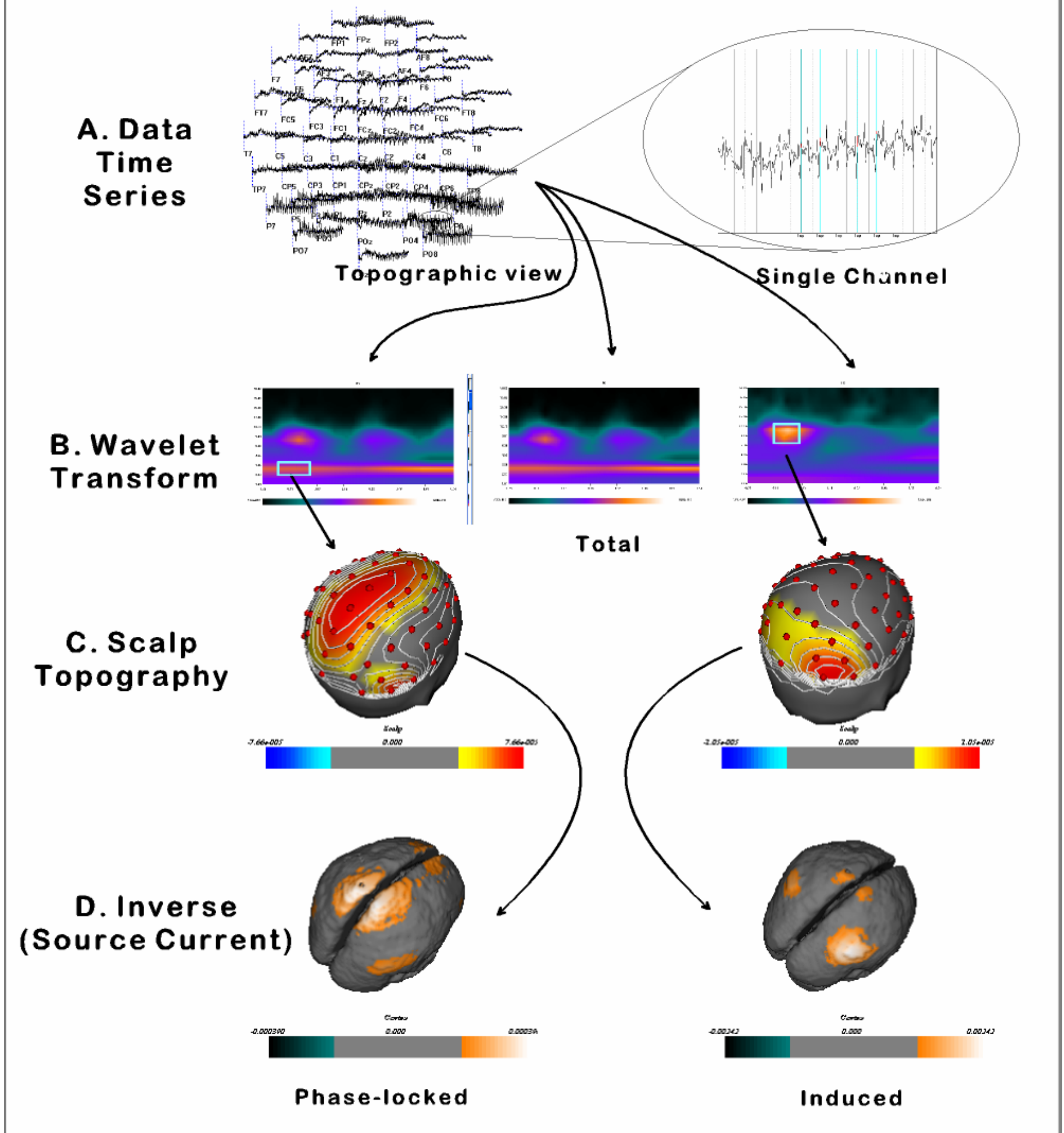


**Figure 3.** (A) 59 channel electrical recordings were obtained from 16 subjects during rhythmic finger tapping. Individual trials were averaged within subjects, and grand averages were obtained. (B) The grand averages were wavelet transformed. A time-frequency window was selected and the resulting scalp topography (C) was used for source estimation. (D) Cortical current source density estimates were computed on the outer surface of an average brain.